

# Kinetic Study of the Hydroxide Ion Attack on and DNA Interaction with High Spin Iron(II) Schiff Base Amino Acid Chelates Bearing ONO Donors<sup>1</sup>

Laila H. Abdel-Rahman, Rafat M. El-Khatib,  
Lobna A. E. Nassr, and Ahmed M. Abu-Dief

Chemistry Department, Faculty of Science, Sohag University, Sohag, 82534 Egypt  
e-mail: ahmed\_benzoic@yahoo.com

Received June 19, 2014

**Abstract**—Kinetic study of some novel high spin Fe(II) complexes of Schiff base ligands derived from 5-bromosalicylaldehyde and amino acids with the OH<sup>-</sup> ion and DNA has been carried out. Based on the kinetic data, the rate law and a plausible mechanism were proposed. Kinetic data of the base catalyzed hydrolysis imply pseudo first-order double stage process due to the presence of mer- and fac-isomers. The observed rate constants  $k_{\text{obs}}$  were correlated with the effect of a substituent R in the structure of ligands. The rate constants and activation parameters are in good agreement with stability constants of the studied complexes. Reactivity of the complexes towards DNA correlated well with the reported binding constants.

**Keywords:** base catalyzed hydrolysis, reactivity, reaction mechanism, thermodynamic parameters, DNA interaction

**DOI:** 10.1134/S1070363214090321

## INTRODUCTION

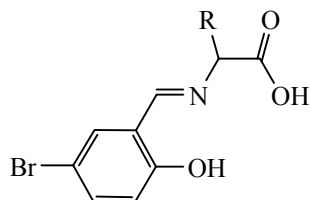
The modern strategy for drugs design is based not entirely on the structure but also the mode of action of a drug towards its specific targets. Schiff base complexes are of high importance as radiotracers [1], biologically active reagents [2–5], catalysts of oxidation [6, 7], epoxidation [8], polymerization [9], and decomposition [10, 11] reactions. Over recent decades considerable attention was paid to a variety of low-spin tris-ligand Fe(II) complexes [12–18]. Influence of substituents on basic hydrolysis of tris-ligand-Fe(II) complexes of Schiff base ligands derived from 2-acetylpyridine and substituted benzylamines and their aniline analogues is presented in the publication [19]. Iron(II) Schiff base complexes provide useful structural and electronic models for the similarly coordinated sites detected in heme iron enzymes. Such complexes are important for the asymmetric oxidation of organic substrates as their structure and catalytic activity are similar to those of iron porphyrins [20]. The present study is devoted to

the hydroxide group attack on some newly produced Schiff base amino acid Fe(II) complexes [21] (Scheme 1).

## EXPERIMENTAL

**Materials and methods for the base hydrolysis reaction.** Iron(II) complexes were synthesized according to the method presented in publications [5, 21, 22]. An aqueous solution of an  $\alpha$ -amino acid was mixed with hot solution of an aldehyde in ethanol. The resulting Schiff base amino acid ligand was stabilized by chelation with Fe(II) by adding an equivalent quantity of aqueous solution of ferrous ammonium sulfate. For avoiding Fe(II) oxidation 5–6 drops of glacial acetic acid were added. The resulting solution was stirred for 9 h under nitrogen. The isolated complexes were recrystallized from water–ethanol solutions. Compositions of the complexes were elucidated by CHN microanalysis, IR, and UV-Vis spectroscopy, and magnetic moments measurements [5]. Purity of the synthesized complexes was detected spectrophotometrically (Table 1). Stability of Fe(II) cation was tested by its resistance to reduction by dithionite. An aged complex solution was treated with NaOH under N<sub>2</sub> and the following formation of green

<sup>1</sup> The text was submitted by the authors in English.

**Scheme 1.** Structures and abbreviations of the Schiff base ligands and abbreviations of their corresponding complexes.

Acronym		R
ligand	complex	
bsal	bsali	CH <sub>3</sub>
bsphal	bsphali	CH <sub>2</sub> C <sub>6</sub> H <sub>5</sub>
bsas	bsasi	CH <sub>2</sub> COOH
bsh	bshi	
bsar	bsari	

**Table 1.** Molecular electronic spectra of the prepared Schiff base amino acid Fe(II) complexes

Schiff base ligands and their complexes	$\lambda_{\max}$ , nm <sup>a</sup>	$\epsilon_{\max}$ , mol <sup>-1</sup> cm <sup>2</sup>	Bands assignment
bsali	398 sh	1310	Intraligand
	440	824	LMCT
	494	900	<i>d-d</i>
bsphali	368 sh	2744	Intraligand
	434	2449	LMCT
	490	2766	<i>d-d</i>
bsasi	376	1252	Intraligand
	438	1332	LMCT
	488	1571	<i>d-d</i>
bshi	368 sh	1765	Intraligand
	428	1518	LMCT
	460	1288	<i>d-d</i>
bsari	370	2350	Intraligand
	430	2383	LMCT
	458 b	2650	<i>d-d</i>

precipitate of Fe(OH)<sub>2</sub> indicated the presence of Fe(II) in the solution of a complex. Deep violet color of the complex solution faded in the course of the reaction. In the course of time the solutions turned colorless with a trace of green colloidal particles of Fe(OH)<sub>2</sub> in there that were slowly growing pale yellow. Eventually, the hydrolysis product precipitated in the form of brown Fe(OH)<sub>3</sub> as a result of oxidation by O<sub>2</sub>. Kinetic studies were carried out with a Jasco UV-Vis spectrophotometer V-530 in 10 mm quartz cells connected with an ultrathermostate (CRIOTERM model 190) by measuring absorbance at  $\lambda_{\max}$  over the period of 2.5 half lives for each run [23–25] with no interference of any reagents at this wavelength. Due to the OH<sup>-</sup> ion concentration being much higher than that of a complex the reaction kinetics was pseudo-first-order. The pseudo-first-order constants were calculated by the least-mean-squares method based on the slopes of the first-order plots as presented in Table 2. The two-stage kinetics deduced from the plots was due to the presence of the labile *cis* and inert *trans* isomers of the octahedral structures [26]. Standard analysis of the absorbance versus time plots presented satisfactory

**Table 2.** Observed first order rate constant<sup>a</sup> ( $k_{\text{obs}} \times 10^4$ , s<sup>-1</sup>) values of basic hydrolysis of bromosalicylidene Schiff base amino acid complexes in aqueous media at various [OH<sup>-</sup>] × 10<sup>-3</sup> mol dm<sup>-3</sup>, [complex] = 1.0 × 10<sup>-4</sup> mol dm<sup>-3</sup>, *I* = 0.01 mol dm<sup>-3</sup> and 298 K

Complex [OH <sup>-</sup> ]	bsali	bsphali	bsasi	bshi	bsari
2.50	5.76	6.78	8.43	7.58	4.28
3.33	7.19	8.22	10.13	9.08	5.57
4.17	8.57	10.06	12.15	10.86	7.21
5.83	11.53	13.12	14.87	13.92	9.62
6.67	12.92	14.76	16.61	15.56	11.03
7.50	14.38	16.23	18.51	17.13	12.56
9.17	17.45	19.35	21.65	20.15	15.05
Complex	$k_1 \times 10^4$		$k_2 \times 10^2$		
bsali	1.34		1.34		
bsphali	2.09		2.09		
bsasi	3.61		3.61		
bshi	2.86		2.86		
bsari	0.27		0.27		

<sup>a</sup> Maximum error is 1%.

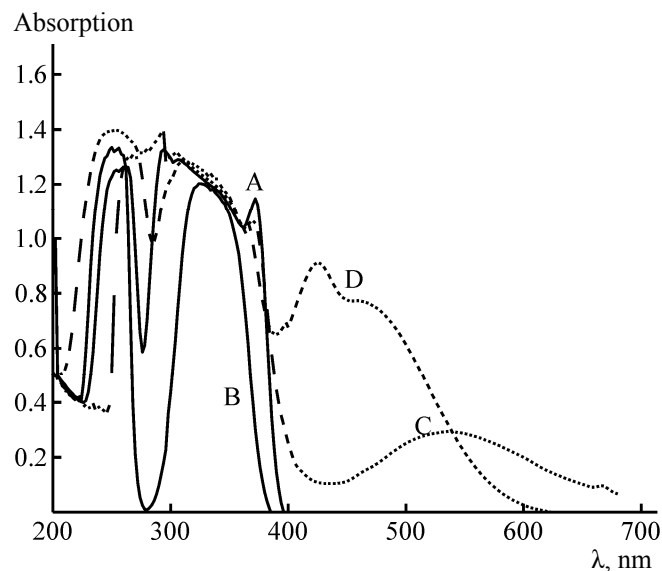


**Fig. 1.** Molecular electronic spectra of bshi complex and its components in ethanol at 298 K. (A)  $1 \times 10^{-3}$  M Brsal, (B)  $1 \times 10^{-3}$  M bsh, (C)  $1 \times 10^{-3}$  M Fe-Brsal, (D)  $6 \times 10^{-4}$  M bshi.

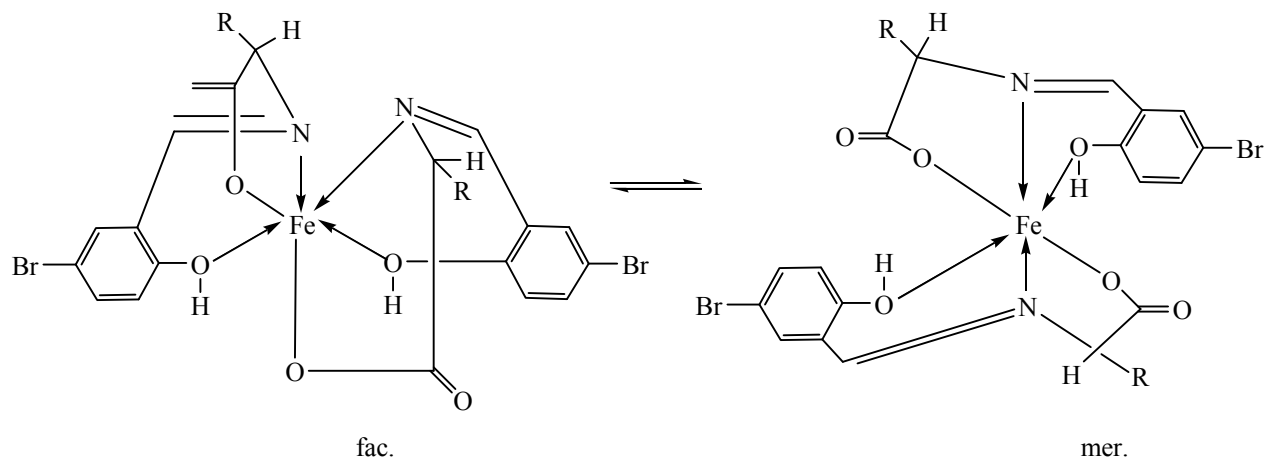
estimates for the slow second-stage rate constant values presented in Table 2. Concentration of NaOH was determined by using the conventional method based on standard oxalic acid. The ionic strength of the solutions was maintained constant at 0.01 M using sodium nitrate. Activation parameters were derived from Arrhenius and Eyring plots ( $T = 283\text{--}313$  K).

Kinetics of interaction of the synthesized complexes with calf thymus DNA was studied with PG UV-Vis spectrophotometer at  $25.0 \pm 1^\circ\text{C}$ .

## RESULTS AND DISCUSSION

In the UV-Vis spectra (Fig. 1) the characteristic band of the complexes was recorded at  $\lambda_{\text{max}} = 458\text{--}494$  nm (Table 1).  $\lambda_{\text{max}}$  of bshi shifted from 504 nm to 485 nm upon addition of the base. The latter band of the complex decayed in accordance with the first-order kinetics. Repeated spectral scans of bshi stood for the first-order kinetics of the base fission in the attacked complex intermediate. Basic hydrolysis of the complexes included a nucleophilic attack by the  $\text{OH}^-$  ion on the complex which afforded free ligand and in the presence of dissolved oxygen gave colloidal Fe(III) hydroxide. The cell content was yellow and optically clear by the end of each run. All complexes provided evidence for the two-stage kinetics. Analyses of absorbance vs. time presented good estimates for the fast and slow stages. The first step of the process corresponded to the parallel basic hydrolysis of the more labile fac isomer and inert mer form. The second stage corresponded to reactivity of the mer form as had been observed earlier [26] (Scheme 2). Vichi and Krumholz reported kinetics for iron(II) complexes derived from pyridine-2-carboxaldehyde and *n*-propylamine. The results were interpreted in terms of parallel first-order processes associated with the break of two iron–nitrogen bonds with different rates in mer and fac isomers [27] that existed in thermodynamic equilibrium in the solutions. Contribution of the first step became lower when a stock solution of the complex was stored for longer periods of time due to hydrolysis of the labile isomer [28]. In our study complexes of the fast isomer were observed for longer

**Scheme 2.** The suggested isomers of the complexes studied (see R in Scheme 1).



time compared to the complexes presented in the publication [28].

**Mechanism of the hydroxide ion attack on iron (II) chelates.** First-order rate constants for the basic hydrolysis ( $k_{\text{obs}}$ ) in aqueous media are cited in Table 2. The plots of  $k_{\text{obs}}$  vs. hydroxide concentration exhibited linear relationship. Equation (1) presents the general rate law used for wide range of the hydroxide ion concentration and ionic strength

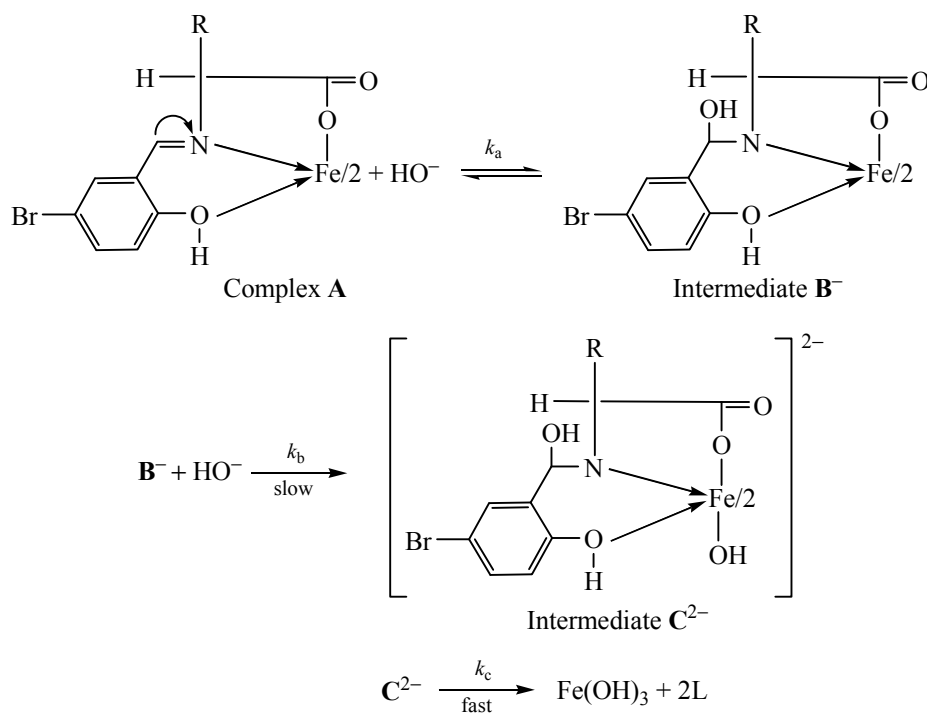
$$\text{Rate} = \frac{-d[\text{complex}]}{dt} = (k_1 + k_2[\text{OH}^-])[\text{complex}]. \quad (1)$$

Here  $k_1$  is the rate constant of dissociation of the complex in neutral solution. The observed  $k_{\text{obs}}$  has the following relationship with the hydroxide ion concentration [29]:

$$k_{\text{obs}} = k_1 + k_2[\text{OH}^-]. \quad (2)$$

Values of  $k_1$  and  $k_2$  order rate constants were calculated by least square method applied to  $k_{\text{obs}}$  vs.  $[\text{OH}^-]$  plots.

Mechanism of basic hydrolysis of the complexes was as follows:



The above mechanism is somewhat similar to that of ruthenium(II) [27] which means a fast pre equilibrium step with one hydroxide ion attacking the electrophilic azomethine carbon atom [30] to form the intermediate  $\mathbf{B}^-$ . Presumably the rate-determining step implies the parallel attack of the hydroxide ion on the central iron atom in the intermediate  $\mathbf{B}^{2-}$  giving the intermediate  $\mathbf{C}^{2-}$  and liberation of the first ligand. The high electron density of the  $t_2g^6$  configuration [31] of Fe(II) in the octahedral chelates retarded the attack of the hydroxide ion on the iron atom.

According to this mechanism the basic hydrolysis rate can be deduced from the steady-state approximation to concentration of the intermediates, as follows:

$$\text{Rate} = \frac{-d[\text{complex}]}{dt} = \frac{k_a k_b k_c [\text{OH}^-][\mathbf{A}]_T}{1 + k_a k_b [\text{OH}^-] + k_a k_c [\text{OH}^-]}, \quad (3)$$

where  $[\mathbf{A}]_T$  is the total analytical concentration of the complex

$$k_{\text{obs}} = \frac{k_a k_b k_c [\text{OH}^-][\mathbf{A}]_T}{1 + k_a k_b [\text{OH}^-] + k_a k_c [\text{OH}^-]}, \quad (4)$$

$$[\mathbf{A}]_T = [\mathbf{A}]_{\text{ss}} + [\mathbf{B}^-]_{\text{ss}} + [\mathbf{C}^{2-}]_{\text{ss}}. \quad (5)$$

The reaction order ( $n$ ) for  $[\text{OH}^-]$  was determined by a least squares procedure based on the slopes of the linear plots of  $\ln(k_{\text{obs}} - k_1)$  vs.  $\ln[\text{OH}^-]$  according to the following equation:

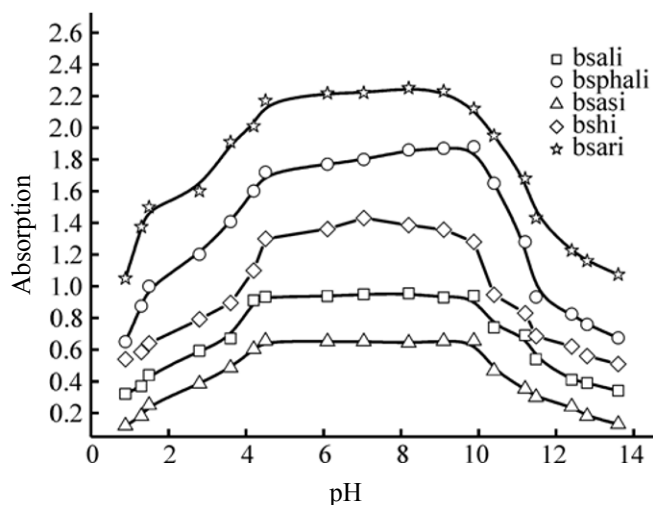


Fig. 2. Dissociation curves of the complexes in aqueous media at complex =  $5 \times 10^{-3}$  M and 298 K.

$$\ln(k_{\text{obs}} - k_1) = \ln k_2 + n \ln [\text{OH}^-]. \quad (6)$$

Calculated values of  $n$  were in the range 0.759–1.013 for the complexes studied.

The dissociation curves of the complexes (Fig. 2) confirmed their resistance towards the hydroxide ion attack within pH range 4 to 10. This correlated well with extremely low  $k_1$  values and the dissociation rate

constant in neutral, weak acidic, and alkaline aqueous solutions of the complexes. Stable violet colour of the solutions within the same pH range also confirmed long term stability of the solutions and, hence, the suggested mechanism of the process at  $\text{pH} > 9$ . The rate of basic hydrolysis increased at higher pH. Reactivity of Fe(II) complexes was controlled predominantly by their hydrophobic and hydrophilic characters. This was deduced from the component rate constant values calculated by least squares method applied to the plots  $k_{\text{obs}}$  versus  $[\text{OH}^-]$  of the complexes. This was ascribed to destabilization of more hydrophobic transient species [30] on one hand, and opposing stabilization of the hydroxide ion in the aqueous media on the other. That explained the highest values of the reaction rate for bsali of low hydrophobic character, and the lowest values for the most hydrophobic bsari species.

**Effect of substituents on reactivity of the studied complexes.** Values of the observed rate constants  $k_{\text{obs}}$  could be correlated with the nature of substituents R in the structures of complexes. Order of reactivity of the complexes towards the hydroxide ion attack increased in the sequence: bsari < bsali < bsphali < bshi < bsasi. This could be related with the inductive effect of a substituent such as higher electron withdrawing

Table 3. Second order rate constant values  $k_2 \times 10^2$ ,  $\text{mol}^{-1} \text{dm}^3 \text{s}^{-1}$  and activation parameters of the basic hydrolysis of bromosalicylidene Schiff base amino acid Fe(II) complexes at different temperatures,  $[\text{complex}] = 1 \times 10^{-4} \text{mol dm}^{-3}$  and ionic strength =  $0.01 \text{mol dm}^{-3}$  in aqueous media

Parameter	Complex				
	bsali	bsphali	bsasi	bshi	bsari
283 K	6.25	6.97	7.78	7.11	5.94
288 K	8.57	9.41	10.24	9.62	8.07
293 K	12.78	14.06	15.65	14.35	12.03
298 K	17.42	18.92	20.63	19.52	16.21
303 K	25.41	27.91	361.05	28.51	23.81
308 K	34.76	37.56	41.13	38.86	32.17
313 K	50.67	–	–	–	47.43
$E_a$ , $\text{kJ mol}^{-1}$	50.03	49.15	47.51	48.25	51.32
$\Delta H^\ddagger$ , $\text{kJ mol}^{-1}$	46.25	45.18	44.27	44.85	48.31
$\Delta G^\ddagger$ , $\text{kJ mol}^{-1}$	82.15	82.14	82.06	82.11	82.71
$\Delta S^\ddagger$ , $\text{J mol}^{-1} \text{K}^{-1}$	–123.16	–127.38	–130.11	–129.38	–116.93
$A \times 10^7$ , $\text{mol}^{-1} \text{dm}^3 \text{s}^{-1}$	8.57	6.42	3.45	5.58	11.68
pK	9.98	9.67	8.86	8.96	10.44

properties of the carboxylic group in bsasi than that of imidazole ring in bshi and phenyl ring in bsphali. In bsari the strong electrons donating guanidine group made reactivity towards the  $\text{OH}^-$  group to be the lowest.

#### Determination of thermodynamic parameters.

Activation parameters of basic hydrolysis were calculated for the complexes by least squares method applied to slopes and intercepts of Arrhenius and Eyring plots (Table 3).  $\text{p}K$  Values of the complexes were determined experimentally by the spectrophotometric continuous variation method [21]. Application of the potentiometric method was retarded by precipitation of iron hydroxide and difficulty in preparing solid amino acid Schiff bases.

Significant negative entropy values of activation (Table 3) supported the proposed mechanism of the reaction that proceeded via formation of an intermediate complex [24, 25]. Various thermodynamic functions were consistent and in good relationship. Such behavior could be ascribed to enhanced stability of the activated complex intermediate.

**Reactivity of the studied complexes towards DNA.** The repeated spectral scans of the reaction of DNA with the complexes were characterized by formation of isosbestic points that confirmed the process taking place (Fig. 3). Values of observed rate constants of the reaction were calculated by the least squares method applied to plots absorbance vs. time (Table 5). Reactivity of the complexes towards DNA was in good agreement with the reported binding constants (Table 5) and had the following relationship:  $\text{bsphali} < \text{bsasi} < \text{bsali} < \text{bshi} < \text{bsari}$ . The rate constant  $k_{\text{obs}}$  for the interaction between CTDNA and the complexes was calculated by plotting  $-\log A$  vs. time (Table 4). The plot of  $k_{\text{obs}}$  versus [DNA] had linear profile typical for pseudo-first order reaction kinetics.

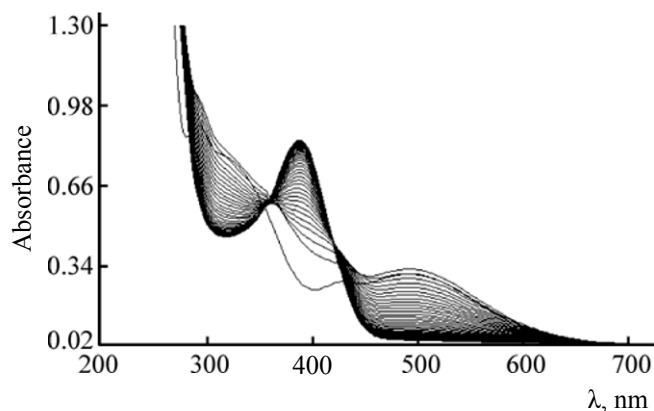


**Fig. 3.** Repeated spectral scans of bsari with CTDNA at  $\text{bsari} = 2 \times 10^{-5} \text{ mol dm}^{-3}$ ,  $\text{CTDNA} = 4 \times 10^{-4} \text{ mol dm}^{-3}$  for 2.5 h, delay time = 4 min.

The second order rate constant values for the reaction of CT-DNA with the complexes were deduced by the least square method applied to  $k_{\text{obs}}$  vs. [DNA] and were correlated well with binding constant values (Table 5).

Linear plots of  $k_{\text{obs}}$  against [DNA] were in good correlation with the following equation:

$$\text{Rate} = \frac{-d[\text{complex}]}{dt} = k_{\text{obs}}[\text{complex}]. \quad (7)$$

The overall rate law for the reaction under conditions of pseudo first order kinetics can be expressed as follows:

$$\text{Rate} = k_{\text{obs}}[\text{complex}] = (k_1 + k_2[\text{DNA}])[\text{complex}]. \quad (8)$$

The  $k_1$  term is assigned to rate determining dissociation of the complexes and the  $k_2$  term to rate determining attack of the compounds by DNA.

**Table 4.** Observed first order rate constant ( $k_{\text{obs}} \times 10^4, \text{s}^{-1}$ ) of interaction of the complexes with CT-DNA at 298 K

Complex	$k_{\text{obs}} \times 10^4, \text{s}^{-1}$				
	2	5	8	11	14
bsali	4.39	5.27	6.10	6.82	7.76
bsphali	3.65	4.27	4.91	5.65	6.21
bsasi	3.91	4.72	5.43	6.02	6.52
bshi	4.65	5.47	6.51	7.60	8.43
bsari	5.03	6.23	7.15	8.12	9.14

**Table 5.** Values of the component rate constant values as calculated by least squares of the plots  $k_{\text{obs}}$  vs. [DNA] of the complexes in aqueous media at [complex] =  $3 \times 10^{-5}$  mol dm<sup>-3</sup> and 298 K

Complex	$k_1 \times 10^4$ , s <sup>-1</sup>	$k_2$ , mol <sup>-1</sup> dm <sup>3</sup> s <sup>-1</sup>	$k_b \times 10^{-4}$ , mol <sup>-1</sup> dm <sup>3</sup>
bsali	3.69	0.30	6.70 ± 0.02
bsphali	3.20	0.15	5.79 ± 0.02
bsasi	3.58	0.25	6.23 ± 0.02
bshi	3.80	0.36	7.04 ± 0.02
bsari	4.44	0.43	10.70 ± 0.02

**Table 6.** The reaction order ( $n$ ) values as calculated by the least squares method applied to the plots  $\ln(k_{\text{obs}} - k_1)$  vs.  $\ln$  [DNA] for the reaction of the complexes with CT-DNA in aqueous media, at [complex] =  $3 \times 10^{-5}$  mol dm<sup>-3</sup> and 298 K

Complex	Reaction order ( $n$ )
bsali	0.91
bsphali	1.03
bsasi	0.93
bshi	1.01
bsari	0.94

**Determination of the reaction order.** Values of the reaction order ( $n$ ) for [DNA] were determined by the least squares method applied to slopes of the linear plots  $\ln(k_{\text{obs}} - k_1)$  vs.  $\ln$  [DNA] in accordance with the following equation:

$$\ln(k_{\text{obs}} - k_1) = \ln k_2 + n \ln [\text{DNA}]. \quad (9)$$

Values of  $n$  indicated that the reaction of CT-DNA with the complexes complied with the first order kinetics in respect to [DNA].

#### REFERENCES

- Luo, H., Fanwick, P.E., and Green, M.A., *Inorg. Chem.*, 1998, no. 37, p. 1127
- Mohamed, G.G., Omar, M.M., and Hindy, A.M.M., *Spectrochim. Acta A*, 2005, no. 62, p. 1140.
- El-Behery, M. and El-Twigry, H., *Spectrochim. Acta A*, 2007, no. 66, p. 28.
- Abdel-Rahman, L.H., El-Khatib R.M., Nassr, L.A.E., Abu-Dief, A.M., and Lashin, F.E., *Spectrochim. Acta*, 2013, no. 111, p. 266.
- Abdel-Rahman, L.H., El-Khatib, R.M., Nassr, L.A.E., Abu-Dief, A.M., Ismael, M., and Seleem, A.A., *Spectrochim. Acta*, 2014, no. 117, p. 366.
- Abbo, H.S., Titinčić, S.J.J., Prasad, R., and Chand, S., *J. Mol. Catal. A: Chem.*, 2005, no. 225, p. 225.
- Gupta, K.S. and Sutar, A.K., *J. Mol. Catal. A: Chem.*, 2007, no. 272, p. 64.
- Shyu, H., Wei, H., Lee, G., and Wang, Y., *J. Chem. Soc., Dalton Trans.*, 2000, p. 915.
- Wu, Z., Xu, D., and Feng, Z., *Polyhedron*, 2001, no. 20, p. 281.
- Nath, M. and Kamaluddin, S., *J. Cheema, Ind. J. Chem. A*, 1993, vol. 32, no. 2, p. 108.
- Gupta, K.S., Abdulkadir, H.K., and Chand, S., *Mol. Catal. A: Chem.*, 2003, no. 202, p. 253.
- Burgess, J. and Prince, R.H., *J. Chem. Soc.*, 1963, p. 5752.
- (a) Burgess, J., *J. Chem. Soc., A*, 1967, p. 431; (b) Burgess, J., *Inorg. Chim. Acta*, 1971, no. 5, p. 133.
- Burgess, J. and Prince, R.H., *J. Chem. Soc.*, 1965, p. 4697.
- Burgess, J. and Prince, R.H., *J. Chem. Soc.*, 1965, p. 6061.
- Burgess, J. Prince, R.H., 1965) *J. Chem. Soc. ., A*, 434.
- Burgess, J., *J. Chem. Soc. A*, 1968, p. 497.
- Krumholz, P., *Struct. Bonding*, 1971, no. 9, p. 139.
- Alshehri, S., Burgess, J., and Shaker, A.M., *Trans Met. Chem.*, 1998, no. 23, p. 689.
- Canali, L. and Sherrington, D.C., *Chem. Soc. Rev.*, 1999, no. 28, p. 85.
- Abdel-Rahman, L.H., El-Khatib, R.M., Nassr, L.A.E., and Abu-Dief, A.M., *J. Mol. Str.*, 2013, no. 1040, p. 9.
- Sharm, P.K. and Dubey, S.N., *Indian J. Chem. A*, 1994, vol. 33, no. 12, p. 1113.
- Abu-Gharib Ezz, A., EL-Khatib, R.M., Nassr, L.A.E., and Abu-Dief, A.M., *Z. Phys. Chem.*, 2011, no. 225, p. 1.
- Abu-Gharib Ezz, A., EL-Khatib, R.M., Nassr, L.A.E. and Abu-Dief, A.M., *J. Korean Chem. Soc.*, 2011, vol. 50, no. 3, p. 346.
- Abu-Gharib Ezz, A., EL-Khatib, R.M., Nassr, L.A.E. and Abu-Dief, A.M., *Kinet. Catal.*, 2012, vol. 53, no. 2, p. 182.
- Blandamer, M.J., Burgess, J., Elvidge, D.L., Guardado, P., Hakin, A.W., Prouse, L.J.S., Radulovic, S., and Russell, D.R., *Transition Met. Chem.*, 1991, no. 16, p. 82.
- Vichi, E.J.S and Kurmholz, P., *J. Chem. Soc., Dalton Trans.*, 1975, p. 1543.
- Alshehri, S., Burgess, J., and Shaker, A.M., *Trans. Met. Chem.*, 1998, vol. 23, p. 689.
- Blandamer, M.J., Burgess, J., Coohson, P., Roberts, D.L., Willings, P., Mekhail, F.M., and Askalani, P., *J. Chem. Soc., Dalton Trans.*, 1978, p. 996.
- Alshehri, S., Blandamer, M.J., Burgess, J., Guardado, P., and Hurbbard, C.D., *Polyhedron*, 1993, vol. 12, no. 5, p. 445.
- Burgess, J., Ellis, G.E., Evans, D.J., Porter, A., Wane, R., and Wyvill, R.D., *J. Chem. Soc. A*, 1971, p. 44.